ORGANOMETALLICS

ARTICLE

pubs.acs.org/Organometallics

The Pauson-Khand Reaction: A Gas-Phase and Solution-Phase Examination Using Electrospray Ionization Mass Spectrometry

Matthew A. Henderson,[†] Jingwei Luo,[†] Allen Oliver,[‡] and J. Scott McIndoe*[,†]

[†]Department of Chemistry, University of Victoria, P.O. Box 3065, Victoria, British Columbia V8W 3V6, Canada

[‡]Department of Chemistry and Biochemistry, University of Notre Dame, 251 Nieuwland Science Hall, Notre Dame, Indiana 46556-5670, United States

Supporting Information

ABSTRACT: A series of dicobalt hexacarbonyl complexes with charged alkyne ligands were prepared to enable the study of the Pauson−Khand reaction using ESI-MS. The hexacarbonyl complexes can be activated in the gas phase through removal of a CO ligand. The resulting pentacarbonyl ions react readily with alkenes, and no discrimination between alkenes was found for this step, indicating that alkene association is not rate determining in the intermolecular reaction. Solution-phase ESI-MS studies on a system set up for intramolecular reactivity revealed only the hexacarbonyl complex as a detectable intermediate, and the reaction was shown to have a large enthalpy and entropy of activation, consistent with ligand dissociation being rate limiting in the reaction.

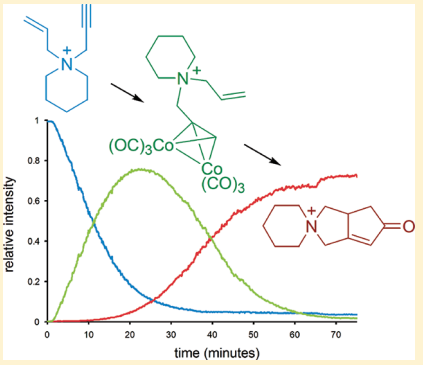

INTRODUCTION

The Pauson-Khand reaction was discovered in 1971 during investigations of the reaction of $Co_2(CO)_8$ with various simple compounds.[1,2] Under a high pressure of CO, an alkene, an alkyne, and CO were observed to combine in a [2 + 2 + 1] cycloaddition reaction to generate a cyclopentenone ring (eq 1).[3] The reaction has since found applications in natural product synthesis, thanks to high stereoselective control and good yields.[4,5]

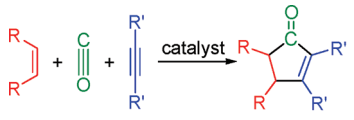

Equation 1

The reaction was initially stoichiometric, yields were generally low, and high pressures of CO and extended reaction times were required.[6,7] Activators that allow less forcing conditions have since been introduced, including amine oxides, cyclohexylamine,[8] sulfides,[9] phosphine oxides,[10] and even water.[11] Catalytic and intramolecular variants are known,[12] and other complexes have shown reactivity, including $Ru_3(CO)_{12}$,[13] several Rh-containing complexes,[14,15] $MoCp_2(CO)_4$,[16] $W(CO)_5(THF)$,[17] $ZrCp_2Cl_2$,[18] and $Fe(CO)_5$.[19,20] The reaction has been performed in ionic liquids, enabling the recycling of the catalyst.[21]

Magnus and co-workers proposed a stoichiometric mechanism based on their observations of the unique stereospecificity characteristic of the cyclization.[22] The related catalytic mechanism (Scheme 1) was proposed in 1990.[23]

Calculations on the reaction profile show a large energy barrier for the formation of **C**, with subsequent reactions occurring rapidly.[24] Efforts have been expended to trap or detect later intermediates.[25] Evans and co-workers were able to crystallize a pentacarbonyldicobalt enyne complex with an (intramolecular) alkene filling the sixth coordination site,[26] but the subsequent insertion reaction failed. Another study employed a chiral cyclopropene complex in an intermolecular reaction with a $Co_2(CO)_6$(alkyne) complex and trapped an inserted byproduct in which the cyclopropene ring had opened.[27] It seems when the alkene binds with a favorable orientation, alkene insertion follows along with CO insertion and subsequent reductive elimination of the product.[28] When the alkene binds in an unfavorable geometry, alkene insertion follows because this reaction is not dependent on the stereochemistry of the alkene, but subsequent CO insertion is prevented, indicating that stereospecificity is dictated by this reaction. In order to satisfy the valencies of both cobalt atoms, the cyclopropene ring opens for anionic coordination of the third carbon atom. Another study with evidence of pentacarbonyl complexes employed alkynes with donor atoms such as sulfur, which displace one CO ligand and trap the coordination site.[29,30]

Although the Pauson−Khand reaction has been around for several decades, there is just one detailed kinetic study, employing (trimethylsilyl)ethyne and norbornadiene (NBD).[31] The authors used reaction progress kinetic analysis[32] to determine the rate ($=k[Co_2(CO)_8]^{1.3}[NBD]^{0.3-1.2}/[CO]^{1.9}$), and two important points are immediately apparent. First of all, the alkyne does not appear in the rate equation at all. This means

Received: August 2, 2011
Published: September 25, 2011

   dx.doi.org/10.1021/om200717r | *Organometallics* 2011, 30, 5471–5479

Scheme 1. Proposed Catalytic Cycle for the Intermolecular Pauson−Khand Reaction

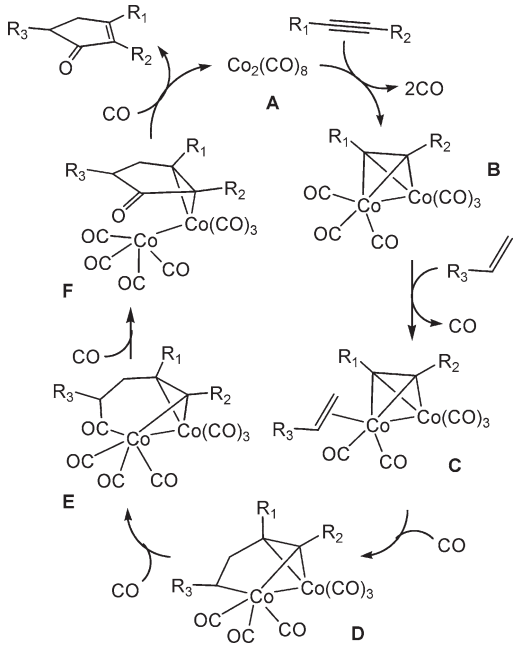

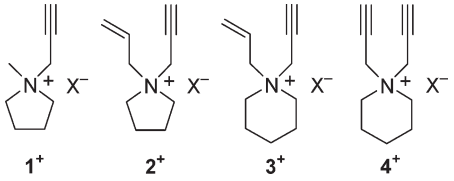

Figure 1. Functionalized pyrrolidinium and piperidinium salts. X^- = Br^-, PF_6^-, BPh_4^-, Tf_2N^-.

that the alkyne is not involved in the rate-determining step, and higher concentrations of alkyne have no effect on the rate of the reaction. Second, added carbon monoxide decreases the reaction rate.

We, and numerous other research groups, are interested in exploiting the unusual speed and sensitivity of ESI-MS to analyze catalytic reactions,[33] but the technique can analyze only ions preformed in solution. With many catalysts being neutral metal complexes,[34] one of the following is required: (a) loss (or gain) of an anionic ligand such as X^-;[35] (b) oxidation of electron-rich metals;[36] (c) association with a charged species such as H^+,[37] Na^+,[38] or Ag^+;[39] (d) deprotonation of an acidic compound;[40] (e) a charged ancillary ligand, most often a phosphine;[41] (f) a charged substrate that imparts its charge to the metal to which it is bound.[42]

The Pauson−Khand reaction has been studied previously by ESI-MS, using the bis(diphenylphosphino)methane (dppm) ligand and phenylacetylene to make $Co_2(CO)_4(DPPM)(\mu_2\text{-}HC_2C_6H_5)$.[43] The methylene of dppm is sufficiently acidic under ESI conditions that it deprotonates to provide an $[M - H]^-$ anionic complex that could be characterized in the negative-ion mode; therefore, this study was an example of approach d.[38] The $[Co_2(CO)_4(DPPM)(\mu_2\text{-}HC_2C_6H_5) - H]^-$ ion was subjected to collisional activation with norbornene gas in the collision cell, and coordination of one alkene moiety was observed after loss of one CO ligand. In this paper, we used approach f and prepared pyrrolidinium and piperidinium salts with an alkyne and/or alkene functionality (Figure 1).[44]

Scheme 2. From Secondary Amine, through Dicobalt Hexacarbonyl Complex, to Cyclopentenone product

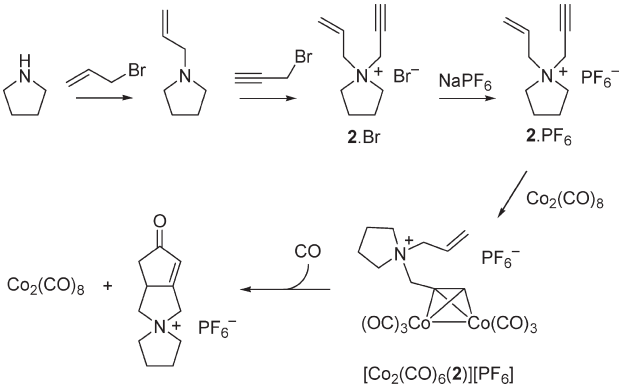

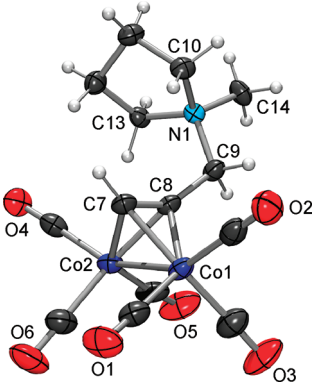

Figure 2. Single-crystal X-ray structure of the cationic part of $[Co_2(CO)_6(\mathbf{1})][BPh_4]$. The tetraphenylborate anion is not shown for the sake of clarity. Key bond lengths (Å): Co1−Co2, 2.461; C7−C8, 1.334; C8−C9, 1.488; 1.311 ± 0.01 Å; Co−C, 1.96 ± 0.01; C−O, 1.13 ± 0.01; Co−CO, 1.81 ± 0.02; C−N, 1.52 ± 0.02. Key bond angles (deg): C6−C7−C8, 146.2; Co−Co−C, 51 ± 1; Co−C−Co, 77.5 ± 0.3.

These salts were prepared in good yield starting from secondary or tertiary amines, and all reacted readily with $Co_2(CO)_8$ in dichloromethane at room temperature to form the corresponding $Co_2(CO)_6(\mu\text{-alkyne})$ complex. The synthetic strategy is exemplified in Scheme 2 for the preparation of $[Co_2(CO)_6(\mathbf{2})][PF_6]$ and, ultimately, the cyclopentenone product $[\mathbf{2} + CO][PF_6]$.

The reactivities of **1**−**4** were examined in different ways and will be dealt with separately.

RESULTS AND DISCUSSION

Charged Alkyne Complexes. $\mathbf{1}^+$ has a single alkyne functional group. As the hexafluorophosphate or tetraphenylborate salt, it reacted smoothly with $Co_2(CO)_8$ to form $[Co_2(CO)_6(\mathbf{1})][X]$ - (X = PF_6, BPh_4), and a single-crystal X-ray structure was obtained for $[Co_2(CO)_6(\mathbf{1})][BPh_4]$ (Figure 2).

Having no additional alkene or alkyne functionality, $[Co_2(CO)_6(\mathbf{1})]^+$ can undergo the Pauson−Khand reaction *inter*molecularly only. We first examined its gas-phase behavior by

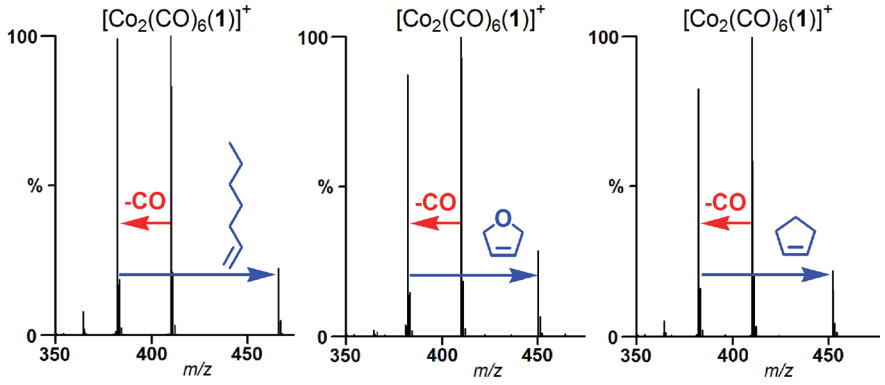

Figure 3. Gas-phase reactions of $[Co_2(CO)_6(\mathbf{1})]^+$ with three different alkenes at a cone voltage of 20 V. In each case, one CO ligand is removed and the alkene adds to $[Co_2(CO)_5(\mathbf{1})]^+$. The alkene does *not* add to the fully saturated ion.

EDESI-MS[45] (see the Supporting Information) to obtain a baseline sense of its reactivity: i.e. how it fragmented under collision-induced dissociation (CID) and what ligands were removed most easily. Loss of six carbon monoxide ligands starts at a relatively low energy (10 V), and all six ligands are gone at approximately 35 V. Free $\mathbf{1}^+$ also begins to appear as a fragment at relatively low voltages, below 25 V. The complexity observed at high energy is the result of a multitude of different fragmentation processes: the Co−Co bond can break to make a $[Co(CO)_x(\mathbf{1})]^+$ complex; N−C bonds can also break to give the methyl pyrrolidinium ion or $[Co_x(CO)_yC_3H_3]^+$ ions; C−H activation of the pyrrolidinium ring is also apparent. However, the high-energy regime is less interesting than what happens at low energies, as the solution reactivity is most likely to mimic the latter. The facile and selective removal of a single CO ligand allowed gas-phase reactions[46] to be conducted, by introducing a volatile alkene (1-hexene, 2,5-dihydrofuran, and cyclopentene) into the source while energizing the ions.

Strained alkenes (such as cyclopentene) are known to react preferentially in the Pauson−Khand reaction, and this has been attributed to a lower energy LUMO.[25] Back-donation from the metal d orbitals into the alkene LUMO is a critical aspect of metallacycle formation (which is also the alkene insertion reaction). Those alkenes with more accessible LUMOs were more reactive. Estimates of reactivity can be made by considering the C=C−C bond angles. Cyclohexene, with an angle of 128°, is sluggish to react, but both norbornene (107°) and cyclopentene (112°) are more reactive.[16c] Alkenes activated by electron-withdrawing groups also show good reactivity.[47]

A qualitative comparison of the reactivity of the cyclopentene system with both 1-hexene (an unstrained alkene) and 2,5-dihydrofuran (a strained and electronically activated alkene) was performed. $[Co_2(CO)_6(\mathbf{1})]^+$ was sprayed into the source conventionally, while the alkene was entrained into the nitrogen desolvation gas. Raising the cone voltage (a means of collisionally activating ions in the source) to 20 V caused loss of one CO ligand, and gas-phase alkene coordination was observed to take place (Figure 3). No dramatic differences in alkene reactivity were observed, even taking into account the different gas-phase concentrations of alkene (which depend on the boiling points; see the Supporting Information). We might expect the reactivities of these alkenes to be similar, given that alkene coordination is independent of the subsequent insertion reaction. As soon as a CO ligand dissociates, alkene coordination is likely to occur quickly, regardless of strain or electronic effects. It is the subsequent insertion reaction that depends on strain or electronic activation.

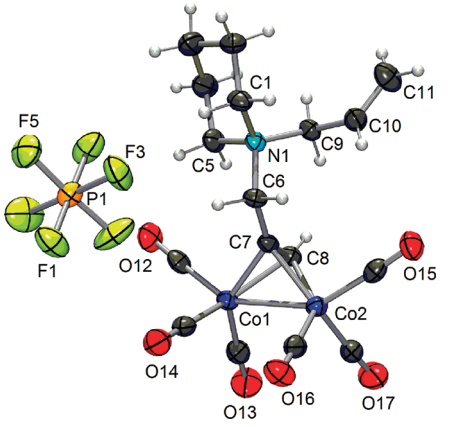

Figure 4. Single-crystal X-ray structure of $[Co_2(CO)_6(\mathbf{3})][PF_6]$. Key bond lengths (Å): Co1−Co2, 2.473; C6−C7, 1.487; C7−C8, 1.336; C10−C11, 1.311; Co−C, 1.96 ± 0.01; C−O, 1.14 ± 0.01; Co−CO, 1.82 ± 0.01; C−N, 1.52 ± 0.01; P−F, 1.60 ± 0.02. Key bond angles (deg): C6−C7−C8, 145.14; C1−N1−C5, 109.74; C9−C10−C11, 121.05; Co−C−Co, 78.2 ± 0.2; Co−Co−C, 50.8 ± 0.2.

The product of the gas phase reaction, $[Co_2(CO)_5(\mathbf{1})(\text{alkene})]^+$, is set up for the Pauson−Khand reaction, having alkyne, alkene, and CO all precoordinated to cobalt. However, MS/MS studies on $[Co_2(CO)_5(\mathbf{1})(\text{alkene})]^+$ invariably regenerated $[Co_2(CO)_5(\mathbf{1})]^+$ (i.e., loss of alkene) as the first fragment (see the Supporting Information). Given that alkenes bind more weakly than CO to low-oxidation-state metals and the insertion is trapped with additional CO, the fact that we were unable to see a complete gas-phase Pauson−Khand transformation is unsurprising.

However, this experimental gas-phase result differs from Gimbert's calculations on the equivalent ion (**C** in Scheme 2),[43] which predicted that it had already undergone the insertion reaction to form **D**. We see no evidence of the insertion reaction having happened, because the first fragmentation of the precursor ion $[Co_2(CO)_5(\mathbf{1})(\text{alkene})]^+$ was alkene loss. Had the insertion step already occurred, CID would have caused simple CO dissociation instead, because the insertion step is effectively irreversible.[24] Therefore, while gas-phase studies show excellent evidence for the identity of intermediate **C**, experimental evidence for intermediate **D** is still lacking.

Charged Enyne Complexes. Constructing a charged substrate with both alkene and alkyne functionality was achieved according to Scheme 2. $\mathbf{3}\cdot PF_6$ reacted smoothly with $Co_2(CO)_8$

dx.doi.org/10.1021/om200717r |*Organometallics* 2011, 30, 5471–5479

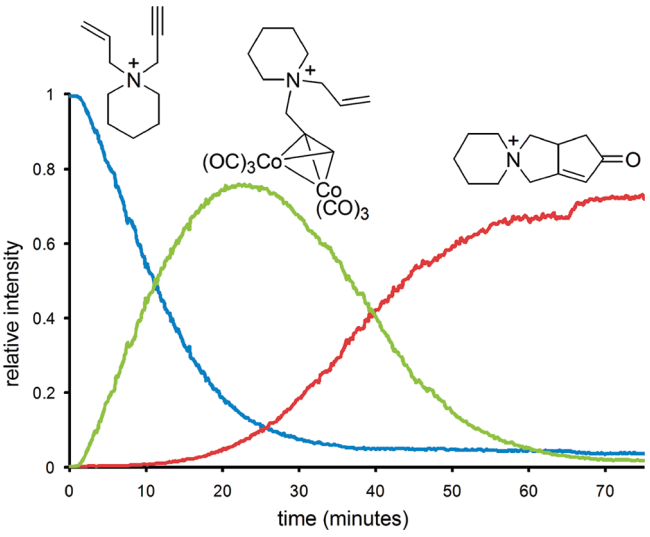

Figure 5. Abundance vs time data for $[\mathbf{3}]^+$ (starting material), $[Co_2(CO)_6(\mathbf{3})]^+$ (intermediate), and $[\mathbf{3} + CO]^+$ (product). Data were collected using positive ion ESI-MS in chlorobenzene, pressurized (with CO gas) sample infusion with online dilution with acetone, and a Schlenk flask saturated with CO before data collection began. Data have been normalized to the total ion current. The scan time was 10 s per spectrum. Approximately 20% of the total ion current at the end of the reaction consisted of numerous low-abundance byproducts, none of which exceeded 5% of the total.

to form $[Co_2(CO)_6(\mathbf{3})][PF_6]$ (analogous reactivity was observed for $\mathbf{2}\cdot PF_6$), and the X-ray crystal structure is shown in Figure 4. Bond lengths and angles are very similar to those of $[Co_2(CO)_6(\mathbf{1})][BPh_4]$. The C=C double bond at 1.311 Å is slightly shorter than the bound alkyne at 1.336 Å, indicating the degree to which the C≡C triple bond is weakened by coordination to the two cobalt centers. The double bond is oriented well away from the metals, consistent with the fact that they are coordinatively saturated. It is not, however, difficult to imagine a conformation in which the alkene is capable of bonding directly to cobalt, provided a coordination site is made available through dissociation of a CO ligand.

Gas-phase reactions of $[Co_2(CO)_6(\mathbf{2})]^+$ and $[Co_2(CO)_6(\mathbf{3})]^+$ were investigated, and as expected, the complexes readily lost CO under CID conditions, analogous to the case for $[Co_2(CO)_6(\mathbf{1})]^+$. Evidence that intramolecular alkene coordination occurred was obtained indirectly, because this transformation does not involve a change in m/z value and is hence invisible to mass spectrometric methods. Cyclopentene was introduced into the source and did *not* react at all with $[Co_2(CO)_5(\mathbf{2})]^+$ or $[Co_2(CO)_5(\mathbf{3})]^+$, implying that the vacant coordination site generated by loss of CO was occupied by the alkene (see the Supporting Information). CID of the cations in the gas phase did not produce any product ions representing the desired product, $[\mathbf{L} + CO]^+$.

However, because all the components of the Pauson–Khand reaction (CO, alkyne, alkene) are present on $[Co_2(CO)_6(\mathbf{3})]^+$, the opportunity existed for a simple solution-phase analysis of the production of $[\mathbf{3}\cdot CO]^+$ from $[\mathbf{3}]^+$. We have recently developed tools for the constant monitoring of reactions under "real" conditions using ESI-MS: namely, pressurized sample infusion (PSI).[48] This approach to reaction monitoring essentially involves a cannula transfer from a solution in a Schlenk flask into the mass spectrometer via narrow-diameter tubing (PEEK chromatography tubing of nominal inner diameter 127 μm), and online dilution can be used to improve spray quality and/or quench the reaction. Overpressures of 1–5 psi are typically used to achieve the desired flow rate (about 10 μL min^{-1}), and dense data may be obtained on the abundance of all charged species in solution, including low-abundance intermediates.[49] For this experiment, we used CO as the pressurizing gas. Because the reaction produces $Co_4(CO)_{12}$ as a byproduct, and this cluster is rather insoluble, we found crystallization of this compound caused the ion current to drop steadily over the course of the reaction and eventually the PEEK tubing would block completely. Spectra were normalized to the total ion current (TIC) to correct for these spray irregularities.

$Co_2(CO)_8$ was added to a chlorobenzene solution of $[\mathbf{3}][Tf_2N]$ under a CO atmosphere and the reaction monitored for 75 min using ESI-MS (Figure 5). The appearance of only one intermediate was observed, the anticipated $[Co_2(CO)_6(\mathbf{3})]^+$. It in turn was consumed, with the appearance of the product, $[\mathbf{3} + CO]^+$. No intermediates were observed in the reaction (i.e., species with more or less than six CO ligands), again consistent with the ligand dissociation step being rate determining.

The reaction was repeated at different temperatures, this time starting with the preprepared complex $[Co_2(CO)_6(\mathbf{3})][Tf_2N]$, which was injected directly into a hot, CO-saturated solution. The reaction was conducted at 65, 70, and 75 °C. Speciation was complicated due to the appearance of aggregates and solvent adducts, but these signals could be combined in a rational way (see Supporting Information) to obtain traces of reaction progress (Figure 6). The rate increases with temperature; the first 20% of the reaction is slow but after that point each trace follows (pseudo) first-order kinetics. Plotting the natural log of the concentration of $[Co_2(CO)_6(\mathbf{3})]^+$ vs time for each experiment produced a plot which was initially curved but that had a straight-line region in the middle (covering conversions from 25% to at least 80%; reactions were stopped when the total ion current dropped too low to obtain good data), with k_{obs} = 0.050, 0.099, and 0.245 s^{-1} at 65, 70, and 75 °C, respectively.

The enthalpy and entropy of activation were determined using an Eyring plot (inset, Figure 6), which provided the activation parameters: $\Delta H^{\ddagger}$ = 150 kJ mol^{-1} and $\Delta S^{\ddagger}$ = 110 J mol^{-1} K^{-1}. These relatively large values are consistent with the rate-determining step being ligand dissociation. They compare with values for $\Delta H^{\ddagger} = 123.6 \pm 11.0$ kJ mol^{-1} and $\Delta S^{\ddagger} = 72.4 \pm 37.3$ J mol^{-1} K^{-1} for the rate of reaction of $Rh_4(CO)_{12}$ with an alkyne, another reaction thought to be limited by dissociation of a CO ligand.[50]

Bis-Alkynes. The reactivity of bis-alkyne compounds is less explored than that for enynes;[51,52] some reports of bis-alkyne complexes employing $Co_2(CO)_8$ are in the bis-cyclopentenone reaction within the same organic moiety (i.e., both alkynes undergo separate *inter*molecular Pauson–Khand reactions without any *intra*molecular interference from the other alkyne).[53,54] In this system, however, the alkyne groups are positioned such that they may react with each other as an alkene and alkyne, as two alkenes, or as two alkynes.

Unlike the case for compounds $[Co_2(CO)_6(L)][PF_6]$ (L = **1**–**3**), it was not possible to isolate the hexacarbonyl complex $[Co_2(CO)_6(\mathbf{4})][PF_6]$ in pure form, because even at room temperature the second alkyne moiety was sufficiently reactive to displace a third CO ligand to form a pentacarbonyl complex (Figure 7).

The occurrence of the pentacarbonyl complex $[Co_2(CO)_5(\mathbf{4})][PF_6]$ in abundance was encouraging, as it represented the possible isolation of an intermediate complex whereby a cyclic

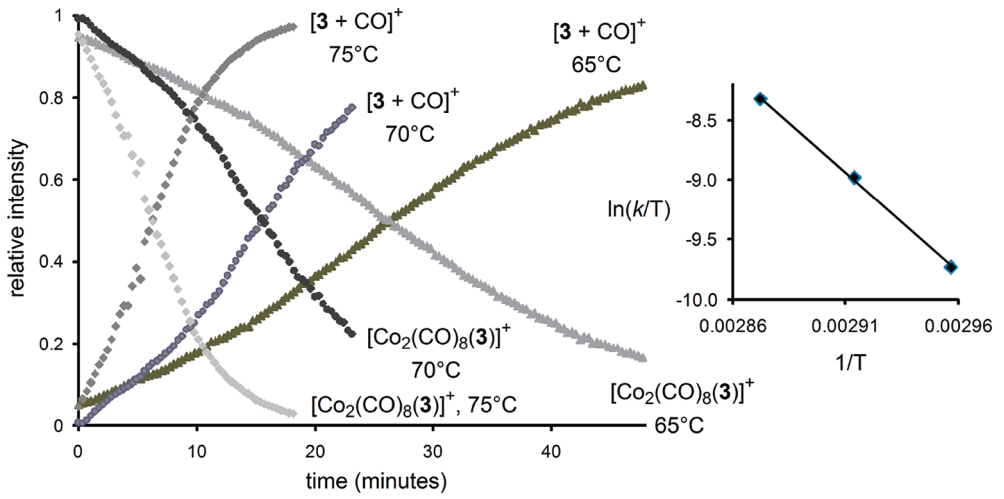

Figure 6. Intensity vs time data for $[Co_2(CO)_6(\mathbf{3})]^+$ (starting material) and $[\mathbf{3} + CO]^+$ (product), collected at three different temperatures. Inset: Eyring plot for the three different temperatures.

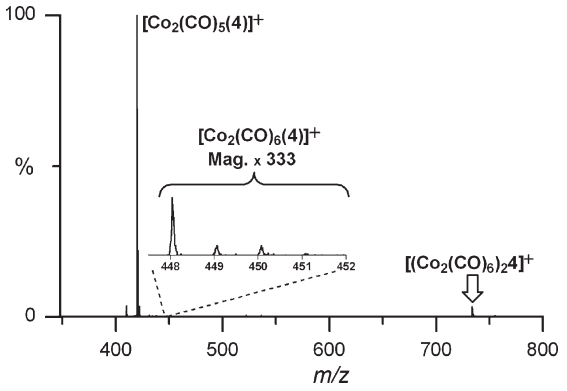

Figure 7. ESI-MS of the reaction between $[\mathbf{4}][PF_6]$ and $Co_2(CO)_8$ in refluxing dichloromethane. After 4 h, $[Co_2(CO)_6(\mathbf{4})]^+$ had almost completely disappeared, to be replaced by $[Co_2(CO)_5(\mathbf{4})]^+$.

product could be reductively eliminated with the same regiochemistry of an intramolecular enyne system.[55] Unfortunately, attempts to crystallize $[Co_2(CO)_5(\mathbf{4})][PF_6]$ produced only crystals of bis(hexacarbonyldicobalt) bis(propargyl)piperidinium hexafluorophosphate, $[\{Co_2(CO)_6\}_2(\mathbf{4})][PF_6]$ (X-ray structure in Figure 8), a minor product observed in the ESI-MS and a possible decomposition product of $[Co_2(CO)_5(\mathbf{4})][PF_6]$. Along with these crystals, a brown powder formed at the bottom of each tube, consistent with an accompanying decomposition product.

Analogous neutral compounds of bis-alkynyl amines have been reported.[56] Bond lengths and angles in this compound are very similar to those observed in the other two structures and are between the two cobalt clusters in this one.

In the absence of crystallographic evidence, we examined the pentacarbonyl complex $[Co_2(CO)_5(\mathbf{L})][PF_6]$ in solution using other spectroscopic techniques and compared the data to those for the other complexes. The IR spectra of the metal complexes (Table 1) correlated well with literature data.[37] For complexes $[Co_2(CO)_6(\mathbf{L})][PF_6]$ ($\mathbf{L} = \mathbf{1}^+$–$\mathbf{3}^+$) four bands were visible in the terminal bonding region. As reported for neutral enyne complexes,[57] the alkene group does not displace a CO ligand and occupy a coordination site on the metal complex. The spectrum of $[Co_2(CO)_5(\mathbf{4})][PF_6]$ was slightly different, as it had an additional broad absorption at 1983 cm^{-1} indicative of a bridging carbonyl ligand[37] and the 2105 cm^{-1} band was shifted to 2099 cm^{-1}.

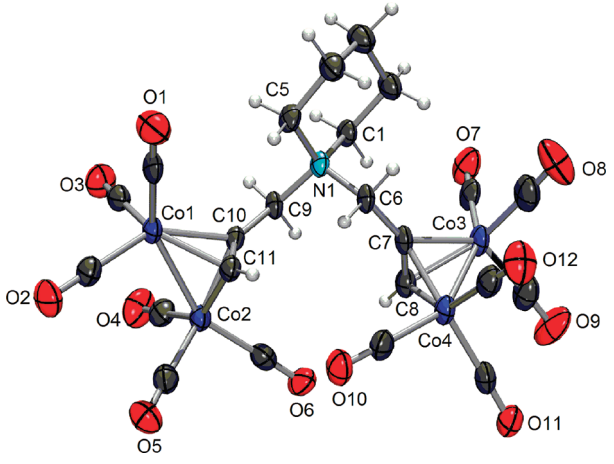

Figure 8. Single-crystal X-ray structure of the cationic part of $[(Co_2(CO)_6)_2(\mathbf{4})][PF_6]$. The hexafluorophosphate anion is not shown for the sake of clarity. Key bond lengths (Å): Co1–Co2, 2.456; Co3–Co4, 2.463; C7–C8, 1.328; C10–C11, 1.336; C9–C10, 1.488; C6–C7, 1.480; 1.311 ± 0.01 Å; Co–C, 1.96 ± 0.01; C–O, 1.13 ± 0.01; Co–CO, 1.81 ± 0.02; C–N, 1.52 ± 0.02. Key bond angles (deg): C9–C10–C11, 146.1; C6–C7–C8, 147.0; Co–Co–C, 51 ± 1; Co–C–Co, 77.5 ± 0.3.

The UV–vis spectra of complexes $[Co_2(CO)_6(\mathbf{L})][PF_6]$ ($\mathbf{L} = \mathbf{1}^+$–$\mathbf{3}^+$) are quite similar (Table 2 and Figure 9). $[Co_2(CO)_5(\mathbf{4})][PF_6]$ was subtly different, having a blue shift of the peak in the visible region and lacking a peak in the region of 360 nm, supporting the notion that the coordination sphere of this complex is distinctly different from those of the other three complexes.

As was the case for $[Co_2(CO)_6(\mathbf{L})][PF_6]$ ($\mathbf{L} = \mathbf{2}, \mathbf{3}$), CID in the gas phase did not lead to production of $[\mathbf{4} + CO]^+$ from $[Co_2(CO)_6(\mathbf{4})]^+$ (see the Supporting Information).

CONCLUSIONS

Our investigations support the notion that the rate-determining step of the intramolecular Pauson–Khand reaction is CO

Table 1. IR Frequencies (cm^{-1})[a]

complex	terminal CO	bridging CO
$[Co_2(CO)_6(\mathbf{1})][PF_6]$	2105 (st), 2067 (vs), 2045 (vs), 2027 (sh)	
$[Co_2(CO)_6(\mathbf{2})][PF_6]$	2105(st), 2067 (vs), 2045 (vs), 2034 (sh)	
$[Co_2(CO)_6(\mathbf{3})][PF_6]$	2105 (st), 2066 (vs), 2045 (vs), 2033 (sh)	
$[Co_2(CO)_5(\mathbf{4})][PF_6]$	2099 (st), 2066 (m), 2044 (vs), 2027 (sh)	1983 (st, broad)

[a] All spectra were run in dichloromethane.

Table 2. UV−Vis Peaks for Cobalt Complexes

complex	peak, nm
$[Co_2(CO)_6(\mathbf{1})][PF_6]$	356, 364, 421
$[Co_2(CO)_6(\mathbf{2})][PF_6]$	356, 365, 421
$[Co_2(CO)_6(\mathbf{3})][PF_6]$	356, 364, 421
$[Co_2(CO)_5(\mathbf{4})][PF_6]$	405

dissociation. Gas-phase studies on the early steps in the reaction scheme showed that CO dissociation and alkene coordination can both be readily achieved and that the coordination of alkene is insensitive to the nature of the alkene, suggesting that the effect of the nature of the alkene operates on some later step in the reaction. Gas-phase investigation of an complex set up for intramolecular reactivity showed circumstantial evidence for alkene coordination, in that complexes activated by CO dissociation were unreactive toward intermolecular alkene association. The reaction could not be driven to completion in the gas phase, probably due to the absence of CO required to trap the inserted intermediates and hence promote further steps. Turning to the solution phase, the intramolecular reaction could be monitored using PSI-ESI-MS and no intermediates apart from the dicobalt hexacarbonyl ion were observed, suggesting that the later steps in the reaction are relatively fast. Positive values of $\Delta H^{\ddagger}$ and $\Delta S^{\ddagger}$ suggest that the rate-determining step is ligand dissociation, consistent with early loss of CO that allows the alkene to coordinate and the rest of the reaction to proceed.

EXPERIMENTAL SECTION

All solvents were dispensed from an MBRAUN solvent purification system and used within minutes. Inert-atmosphere techniques were used for all syntheses involving $Co_2(CO)_8$. Reagents were purchased from Aldrich and used without subsequent purification. UV−vis spectra were collected on an Agilent 8453 UV−vis spectrometer, and IR spectra were collected on a Perkin-Elmer FT-IR spectrum 1000 instrument.

For the X-ray diffraction studies, arbitrary spheres of data were collected for the samples on a Bruker APEX-II diffractometer using a combination of ω and φ scans of 0.5°.[58] Data were corrected for absorption and polarization effects and analyzed for space group determination.[59] The structures were solved by direct methods and expanded routinely.[60] The models were refined by full-matrix least-squares analysis of F^2 against all reflections. All non-hydrogen atoms were refined with anisotropic thermal displacement parameters. Unless otherwise noted, hydrogen atoms were included in calculated positions. Thermal parameters for the hydrogens were tied to the isotropic thermal parameter of the atom to which they are bonded (1.5× for methyl, 1.2× for all others). Crystal structure depictions were created using Ortep-3[61] and Povray.[62]

All mass spectra were collected by using a Micromass Q-ToF *micro* mass spectrometer in positive ion mode using pneumatically assisted electrospray ionization: capillary voltage, 2900 V; extraction voltage, 0.5 V; source temperature, 80 °C; desolvation temperature, 150 °C; cone gas flow, 100 L/h; desolvation gas flow, 100 L/h; collision voltage, 2 V (for MS experiments); collision voltage, 2−40 V (for MS/MS experiments); low and high mass resolution, 10.0; MCP voltage, 2700 V. Gas-phase ion−molecule reactions were carried out by a published method.[46]

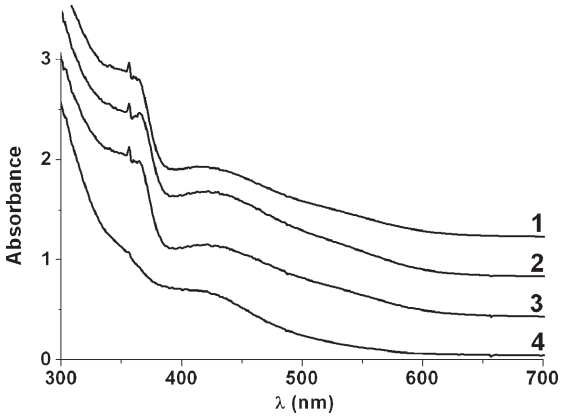

Figure 9. UV/vis spectra of $[Co_2(CO)_6(\mathbf{L})][PF_6]$ ($\mathbf{L}$ = **1**−**3**) and $[Co_2(CO)_5(\mathbf{4})][PF_6]$ (from top to bottom).

1·Br. Methylpyrrolidine (3.84 g, 45.1 mmol) and diethyl ether (30 mL) were cooled to 0 °C in a 100 mL round-bottom flask. Propargyl bromide (5 mL of an 80% solution in toluene, 6.90 g, 57.5 mmol) in ether (25 mL) was added dropwise. The mixture was subsequently warmed to room temperature and stirred overnight. The solvent was then evaporated and the white product dried under vacuum for 24 h (8.97 g, 44.0 mmol, 97%). Mp: 62−68 °C. ^{1}H NMR (CD_3OD): δ (ppm) 4.50 (d, 2H, CH_2-d); 3.75 (m, 4H, CH_2-b); 3.52 (t, 1H, CH-f); 3.29 (s, 3H, CH_3-a); 2.31 (m, 4H, CH_2-c). ^{13}C NMR (CD_3OD): δ (ppm) 81.96 (e); 73.33 (f); 65.25 (b); 54.50 (d); 50.44 (a); 23.20 (c).

1·PF$_6$. An aqueous solution (20 mL of H_2O) of **1**·Br (1.413 g, 6.96 mmol) and sodium hexafluorophosphate (1.19 g, 7.08 mmol) was prepared. The mixture was heated to facilitate dissolution and then cooled to room temperature. The white crystals were filtered with a cold water wash and dried overnight under vacuum (0.62 g, 2.30 mmol, 33%). Mp: 146−147 °C. ^{1}H NMR (CD_3OD): δ (ppm) 4.33 (d, 2H, CH_2-d); 3.67 (m, 4H, CH_2-b); 3.45 (t, 1H, CH-f); 3.22 (s, 3H, CH_3-a); 2.28 (m, 4H, CH_2-c). ^{13}C NMR (CD_3OD): δ (ppm) 81.78 (e); 73.05 (f); 65.15 (b); 54.27 (d); 50.24 (a); 23.08 (c). ^{31}P NMR (CD_3OD): δ (ppm) −143.22 (septet for PF_6^-).

1·BPh$_4$. A 5 mL aqueous solution of **1**·Br (0.102 g, 0.502 mmol) was added to a 5 mL aqueous solution of sodium tetraphenylborate (0.161 g, 0.470 mmol) and stirred for 15 min. A white product formed immediately. An extra 5 mL of water was added to enhance stirring. The product (0.183 g, 0.413 mmol, 87.8%) was collected by vacuum filtration with a wash of water. Dec pt: >200 °C. ^{1}H NMR (CD_3CN): δ (ppm) 7.31 (m, 8H, CH-i); 7.05 (t, 8H, CH-h); 6.87 (t, 4H, CH-j); 4.11 (d, 2H, CH_2-d); 3.53 (m, 4H, CH_2-b); 3.14 (t, 1H, CH-f); 3.14 (s, 3H, CH_3-a); 2.14 (m, 4H, CH_2-c). ^{13}C NMR (CD_3CN): δ (ppm) 165.79 (g), 136.74

(i), 126.60 (h), 122.77 (j), 81.47 (f), 72.63 (e), 65.09 (b), 54.29 (d), 50.58 (a), 22.77 (c).

Allyl Pyrrolidine.[63]. Allyl bromide (6 mL, 8.4 g, 69.4 mmol) in diethyl ether (20 mL) was added dropwise to pyrrolidine (5.1 g, 71.7 mmol) in ether (20 mL) at 0 °C over 30 min. The solution was then warmed to room temperature and stirred overnight, followed by a potassium hydroxide extraction (3 × 25 mL of a 3 M solution). The subsequent aqueous phase was then extracted with dichloromethane and all organic portions were combined, dried with anhydrous magnesium sulfate, and filtered. The solvent was removed on the rotary evaporator, and the orange liquid was distilled (the fraction that boiled at 120 °C was retained) to give a colorless product (3.5 g, 31.5 mmol, 45%). ^{1}H NMR ($CDCl_3$): δ (ppm) 5.88 (m, 1H); 5.21 (m, 2H); 3.02 (d, 2H); 2.43 (m, 4H); 1.71 (m, 4H). ^{13}C NMR ($CDCl_3$): δ (ppm) 136.23, 116.53, 59.22, 53.96, 23.40.

2·Br. Allyl pyrrolidine (0.667 g, 6.00 mmol) and propargyl bromide (0.80 mL, 1.07 g, 7.19 mmol) were stirred in ether (30 mL) overnight. The white product was filtered and collected (0.453 g, 1.86 mmol, 31%). Mp: 140−146 °C. ^{1}H NMR (CD_3OD): δ (ppm) 6.11 (m, 1H, CH-b); 5.76 (m, 2H, CH_2-a); 4.30 (s, 2H, CH_2-f); 4.16 (d, 2H, CH_2-c); 3.68 (m, 4H, CH_2-d); 3.49 (t, 1H, CH-h); 2.28 (m, 4H, CH_2-e). ^{13}C NMR (CD_3OD): δ (ppm) 129.40 (a); 126.55 (b); 82.03 (h); 73.04 (g); 64.55 (c); 63.10 (d); 51.25 (f); 23.22 (e).

2·PF$_6$. An aqueous solution of **2**·Br (0.265 g, 1.16 mmol, 20 mL of H_2O) was added to an aqueous solution of sodium hexafluorophosphate (0.208 g, 1.24 mmol, 10 mL of H_2O). The mixture was reduced to a volume of 10 mL and left overnight in the refrigerator at 5 °C. The white crystals were filtered with a water wash, and the filtrate was then reduced again to a smaller volume and transferred back into the refrigerator for further crystallization. The combined yield of both aliquots was 0.092 g, 0.312 mmol, 27%. Mp: 78−80 °C. ^{1}H NMR (CD_3OD): δ (ppm) 5.96 (m, 1H, CH-b); 5.70 (m, 2H, CH_2-a); 4.15 (d, 2H, CH_2-f); 4.01 (d, 2H, CH_2-c); 3.55 (m, 4H, CH_2-d); 3.36 (t, 1H, CH-h); 2.16 (m, 4H, CH_2-e). ^{13}C NMR (CD_3OD): δ (ppm) 129.37 (a); 126.43 (b); 81.96 (h); 72.95 (g); 64.53 (c); 63.03 (d); 51.10 (f); 23.13 (e). ^{31}P NMR (CD_3OD): δ (ppm) −143.23 (septet).

Allyl Piperidine. Allyl bromide (15.6 g, 128.9 mmol), piperidine (10.5 g, 123.3 mmol), and sodium hydride (3.3 g, 145.9 mmol) were combined as described in the literature to yield allyl piperidine (11.9 g, 95.0 mmol, 77%) after a partial dynamic vacuum distillation. ^{1}H NMR ($CDCl_3$): δ (ppm) 5.82 (m, 1H); 5.05 (m, 2H); 2.89 (d, 2H); 2.30 (s, 4H); 1.52 (m, 4H); 1.37 (m, 2H). ^{13}C NMR ($CDCl_3$): δ (ppm) 135.5, 117.33, 62.56, 54.37, 25.86, 24.26.

3·Br. Propargyl bromide (2.42 g of an 80% solution in toluene, 16.2 mmol) in toluene (20 mL) was added to allyl piperidine (1.94 g, 15.5 mmol) in toluene (20 mL). The mixture was stirred at room temperature for 48 h, and the resulting white product was vacuum filtered, followed by vacuum drying overnight. (2.47 g, 10.1 mmol, 67%). Mp: 154−156 °C. ^{1}H NMR (CD_3CN): δ (ppm) 5.99−5.70 (m, 3H, CH-a, b); 4.43 (d, 2H, CH_2-g); 4.15 (d, 2H, CH_2-c); 3.53 (m, 4H, CH_2-d); 3.27 (t, 1H, CH-i); 1.91 (m, 4H, CH_2-e); 1.69 (m, 2H, CH_2-f). ^{13}C NMR (CD_3CN): δ (ppm) 129.88 (a); 125.01 (b); 82.68 (c); 71.77 (g); 62.33 (h); 59.23 (d); 50.38 (i); 21.39 (f); 20.31 (e).

3·PF$_6$. To 30 mL of water was added **3**·Br (0.45 g, 1.85 mmol) and sodium hexafluorophosphate (0.37 g, 2.20 mmol). The mixture was stirred for 15 min, and the white product was filtered (0.216 g). The filtrate was boiled to reduce the volume down to 15 mL and transferred to the freezer (−10 °C) for 4 h. These crystals were then filtered (0.171 g) to give a combined yield of 0.387 g, 1.25 mmol, 68%. Mp: 85−86 °C. ^{1}H NMR (CD_2Cl_2): δ (ppm) 5.76 (m, 3H, CH-a,b); 3.99 (d, 2H, CH_2-g); 3.95 (d, 2H, CH_2-c); 3.36 (m, 4H, CH_2-d); 2.85 (t, 1H, CH-i); 1.86 (m, 4H, CH_2-e); 1.70 (q, CH_2-f). ^{13}C NMR (CD_2Cl_2): δ (ppm) 131.46 (a); 122.74 (b); 82.22 (c); 70.17 (g); 62.73 (h); 59.22 (d); 49.45 (i); 20.90 (f); 20.15 (e). ^{31}P NMR (CD_2Cl_2): δ (ppm) −143.82 (septet).

Propargyl Piperidine. Piperidine (7.5 mL, 6.5 g, 75.9 mmol) in tetrahydrofuran (50 mL) was added to a slurry of sodium hydride (2.05 g, 85.5 mmol) in tetrahydrofuran (75 mL) over 1 h. The mixture was stirred at room temperature for another 1 h. A mixture of propargyl bromide (9.93 g of an 80% toluene solution, 66.2 mmol) in tetrahydrofuran was then added dropwise over 1 h, and the mixture was stirred overnight. The mixture was quenched with a sodium chloride solution (1 mol L^{-1}) and the organic phase separated. The aqueous phase was then extracted with ethyl acetate (3 × 50 mL) followed by tetrahydrofuran (2 × 50 mL) and combined with the original organic fraction. After drying with anhydrous magnesium sulfate and filtering with a THF wash, the solvent was removed on a rotary evaporator and the orange product distilled to give a light yellow liquid (5.41 g, 43.9 mmol, 66%). ^{1}H NMR ($CDCl_3$): δ (ppm) 4.24 (t, 1H); 3.16 (d, 2H); 2.39 (m, 4H); 1.51 (m, 4H); 1.34 (m, 2H). ^{13}C NMR ($CDCl_3$): δ (ppm) 72.80, 68.36, 52.98, 47.43, 25.73, 23.74.

4·Br. Propargyl piperidine (1.00 g, 8.1 mmol) was added to propargyl bromide (1.38 g of an 80% toluene solution, 9.2 mmol) along with toluene (30 mL), and the mixture was stirred at room temperature for 24 h. The solution was then refluxed for 1 h, and the brown product was vacuum filtered with a toluene wash and dried under vacuum overnight (0.839 g, 3.5 mmol, 43%). Mp: 200 °C dec. ^{1}H NMR (CD_3OD): δ (ppm) 2.73 (d, 4H, CH_2-c); 1.91 (t, 4H, CH_2-d); 1.57 (t, 2H, CH-a); 0.23 (m, 4H, CH_2-e); 0.02 (m, 2H, CH_2-f). ^{13}C NMR (CD_3CN): δ (ppm) 83.00 (c); 71.09 (a); 59.45 (d); 51.01 (b); 21.19 (f); 20.29 (e).

4·PF$_6$. This complex was prepared as for **1**·PF_6 with the following amounts of reagents and solvents: **4**·Br (0.166 g, 0.689 mmol), sodium hexafluorophosphate (0.18 g, 1.07 mmol), water (30 mL). Isolated product: 0.0799 g, 0.26 mmol, 38%. Mp: 160−161 °C. ^{1}H NMR (CD_3OD): δ (ppm) 4.46 (s, 4H, CH_2-c); 3.62 (t, 4H, CH_2-d); 3.53 (t, 2H, CH-a); 1.97 (m, 4H, CH_2-e); 1.74 (m, 2H, CH_2-f). ^{13}C NMR (CD_3OD): δ (ppm) 83.39 (c); 71.33 (a); 59.90 (d); 51.05 (b); 21.81 (f); 20.68 (e). ^{31}P NMR (CD_3OD): δ (ppm) −143.24 (septet).

4·BPh$_4$. A 20 mL aqueous solution of **4**·Br (0.37 g, 1.53 mmol) was added to a 20 mL aqueous solution of sodium tetraphenylborate (0.60 g, 1.75 mmol) and the mixture stirred for 20 min. The white product (0.578 g, 1.20 mmol, 78%) was vacuum filtered with a water wash. X-ray-quality crystals were grown by the slow evaporation of an acetone solution. Mp: 134−136 °C. ^{1}H NMR (CD_3CN): δ (ppm) 7.19 (m, 8H, CH-i); 6.91 (t, 8H, CH-h); 6.76 (t, 4 h, CH-j); 4.15 (d, 4H, CH_2-c); 3.36 (t, 4H, CH_2-d); 3.11 (t, 2H, CH-a); 1.86 (m, 4H, CH_2-e); 1.76 (m, 2H, CH_2-f). ^{13}C NMR (CD_3CN): δ (ppm) 163.8 (g), 135.42 (i), 125.26 (h), 121.46 (j), 81.83 (a), 69.57 (b), 58.47 (d), 49.81 (c), 19.89 (f), 18.96 (e).

[Co$_2$(CO)$_6$(1)][PF$_6$]. Dicobalt octacarbonyl (0.207 g, 0.604 mmol) and **1b** (0.122 g, 0.45 mmol) were mixed as solids in a Schlenk flask. Dry dichloromethane was then added (10 mL), and the mixture was stirred at room temperature for 4 h under N_2. The solvent was evacuated, and the mixture was washed with ether (4 × 8 mL). The red solid was then dried under vacuum for 2 h and collected (0.068 g, 0.122 mmol, 27%). Mp: 120 °C dec. ^{1}H NMR (CD_2Cl_2): δ (ppm) 6.32 (s, 1H); 4.77, (s, 2H); 3.59 (m, 4H); 3.13 (s, 3H); 2.25 (s, 4H). ^{13}C NMR (CD_2Cl_2): δ (ppm) 75.09, 67.67, 65.03, 49.50, 22.16. ^{31}P NMR (CD_2Cl_2): δ (ppm) −143.79 (septet). IR (cm^{-1}, CH_2Cl_2): 2105 (st), 2067 (vs), 2045 (vs), 1605 (m, broad). UV−vis (nm): 356, 364, 421.

[Co$_2$(CO)$_6$(1)][BPh$_4$]. Dicobalt octacarbonyl (1.06 g, 3.10 mmol) was weighed out in a Schlenk flask in the glovebox and transferred to the Schlenk line. **1**·Ph_4 (1.01 g, 2.26 mmol) was then added as a solid, followed by dichloromethane (40 mL). The reaction mixture was stirred at room temperature and tracked by ESI-MS. After about 4 h, the reaction was stopped. Solvent was evaporated under vacuum, and the remaining solid was washed successively with 10 mL portions of dry diethyl ether until the washings were colorless. The dark product was

dried under vacuum overnight and then collected in air (0.996 g, 1.36 mmol, 60%). X-ray-quality crystals were grown by solvent diffusion of dichloromethane and diethyl ether at −10 °C; a thin layer of 1-butanol was put between the two solvents to slow diffusion. This product decomposed quickly in the solid state and was only characterized by X-ray crystallography.

$[Co_2(CO)_6(2)][PF_6]$. Dicobalt octacarbonyl (0.0917 g, 0.268 mmol) was weighed out in a Schlenk flask in a glovebox and then transferred to the Schlenk line, to which **2b** (0.0435 g, 0.147 mmol) was added as a solid. Dry dichloromethane was then added against a stream of nitrogen, and the mixture was stirred at room temperature for 2 h. The solvent was then evacuated and the remaining solid was washed with dry diethyl ether (4 × 6 mL). The remaining solid was then dried under vacuum for 2 h and collected (0.0595 g, 0.102 mmol, 69%). Mp: 80 °C dec. ^{1}H NMR (CD_2Cl_2): δ (ppm) 6.36 (s, 1H); 5.79 (m, 3H); 4.67 (s, 2H); 3.96 (d, 2H); 3.56 (m, 4H); 2.21 (m, 4H). ^{13}C NMR (CD_2Cl_2): δ (ppm) 130.42, 124.09, 63.87, 62.56, 62.14, 22.35. ^{31}P NMR (CD_2Cl_2): δ (ppm) −143.83 (septet). IR (cm^{-1}, CH_2Cl_2): 2105 (st), 2067 (vs), 2045 (vs), 2034 (shoulder). UV−vis (nm): 356, 365, 421.

$[Co_2(CO)_6(3)][PF_6]$. Dicobalt octacarbonyl (0.15 g, 0.439 mmol) and **3b** (0.087 g, 0.281 mmol) were added to a Schlenk flask as solids against a dry nitrogen atmosphere. Dry dichloromethane (10 mL) was then added, and the mixture was allowed to react for 2 h. The solvent was then evaporated, and the red solid was washed with ether (3 × 8 mL) and then dried under vacuum for 2 h. The dark red product (0.131 g, 0.220 mmol, 78%) was collected, and X-ray-quality crystals were grown by dichloromethane and ether solvent diffusion in the freezer, with a small layer of 1-butanol between them. Mp: 90 °C dec. ^{1}H NMR (CD_2Cl_2): δ (ppm) 6.38 (s, 1H); 5.74 (m, 3H); 4.70 (s, 2H); 4.00 (d, 2H); 3.42 (m, 4H); 1.88 (m, 4H); 1.72 (m, 2H). ^{13}C NMR (CD_2Cl_2): δ (ppm) 130.91, 122.91, 75.25, 74.03, 62.69, 62.10, 58.86, 20.96, 20.32. ^{31}P NMR (CD_2Cl_2) δ (ppm) −143.79 (septet). IR (cm^{-1}, CH_2Cl_2): 2105 (st), 2066 (vs), 2045 (vs). UV−vis (nm): 356, 364, 421 nm.

$[Co_2(CO)_6(4)][PF_6]$. Dicobalt octacarbonyl (0.0405 g, 0.118 mmol) and **4b** (0.0391 g, 0.127 mmol) were mixed as solids in a Schlenk flask. Dry dichloromethane (8 mL) was added at 0 °C, and the mixture was stirred for 1 h at this temperature before being warmed to room temperature. The solution was stirred overnight at room temperature and then refluxed for 1 h. The solvent was then evacuated, and the solid was washed once with hexane (8 mL) and then ether (2 × 8 mL) followed by drying under vacuum. The red product was then collected in air (0.0523 g, 0.0926 mmol, 79%). Mp: 130 °C dec. ^{1}H NMR (CD_2Cl_2): δ (ppm) 7.20 (s, 2H); 4.40 (m, 4H); 4.05 (m, 2H); 3.58 (m, 2H); 1.85 (m, 4H); 1.70 (m, 2H). ^{13}C NMR (CD_2Cl_2): δ (ppm) 140.92, 129.13, 64.53, 64.23, 63.68, 28.93, 20.79, 20.24, 19.72, −0.01. ^{31}P NMR (CD_2Cl_2): δ (ppm) −143.75 (septet). IR (cm^{-1}, CH_2Cl_2): 2099 (st), 2066 (m), 2044 (vs), 2027 (s), 1983 (m, broad). UV−vis (nm): 405.

ESI-MS Reaction Monitoring Using Pressurized Sample Infusion. A flask with a built-in condenser topped with a J. Young tap and a side arm fitted with a septum was used for these experiments, as described in ref 49. A solution of [**3**][Tf_2N] (0.224 g, 0.50 mM in chlorobenzene) was monitored using this PSI-ESI-MS setup. To this solution was added $Co_2(CO)_8$ (0.228 g, 0.68 mM in chlorobenzene) by syringe through the septum to initiate the reaction. Alternatively, preprepared [$Co_2(CO)_6$(**3**)][Tf_2N] (0.010 g, 0.014 mM) was monitored by ESI-MS at temperatures of 65, 70, and 75 °C. Overpressure in the flask was held at 5 psi throughout all reactions, and the temperature was monitored by a temperature probe inserted into the pressurized flask (thus, the temperature is the real solution temperature). The reaction mixture was diluted online en route to the MS with acetone at 1 mL/h. The solution end of the PEEK tubing was protected with a standard cannula filter system to avoid the tube being blocked by insoluble byproduct. Data were processed by normalizing the abundance of each species to the total ion count of all species in the spectrum.

■ ASSOCIATED CONTENT

Supporting Information. Figures giving MS data and tables and CIF files giving data for the crystal structure determinations. This material is available free of charge via the Internet at http://pubs.acs.org.

■ AUTHOR INFORMATION

Corresponding Author
*E-mail: mcindoe@uvic.ca.

■ REFERENCES

(1) Khand, I. U.; Knox, G. R.; Pauson, P. L.; Watts, W. E. *Chem. Commun.* **1971**, 36.
(2) Khand, I. U.; Knox, G. R.; Pauson, P. L.; Watts, W. E. *J. Chem. Soc., Perkin Trans. 1* **1973**, 975–977.
(3) Pauson, P. L. *Tetrahedron* **1985**, *41*, 5855–5860.
(4) Magnus, P.; Principe, L. M.; Slater, M. J. *J. Org. Chem.* **1987**, *52*, 1483–1486.
(5) (a) Blanco-Urgoiti, J.; Anorbe, L.; Perez-Serrano, L.; Dominguez, G.; Perez-Castells, J. *Chem. Soc. Rev.* **2004**, *33*, 32–42. (b) Fletcher, A. J; Christie, S. D. R. *J. Chem. Soc., Perkin Trans. 1* **2000**, 1657–1668. (c) Gibson, S. E.; Mainolfi, N. *Angew. Chem., Int. Ed. Engl.* **2005**, *44*, 3022–3037. (d) Green, J. R. *Curr. Org. Chem.* **2001**, *5*, 809–826.
(6) Khand, I. U.; Knox, G. R.; Pauson, P. L.; Watts, W. E.; Foreman, M. I. *J. Chem. Soc. Perkin Trans. 1* **1973**, 977–981.
(7) Geis, O.; Schmalz, H. G. *Angew. Chem., Int. Ed. Engl.* **1998**, *37* (7), 911–914.
(8) Sugihara, T.; Yamada, M.; Ban, H.; Yamaguchi, M.; Kaneko, C. *Angew. Chem., Int. Ed. Engl.* **1997**, *36*, 2801–2804.
(9) Sugihara, T.; Yamada., M.; Yamaguchi, M.; Nishizawa, M. *Synlett* **1999**, 771–773.
(10) Billington, D. C.; Helps, I. M.; Pauson, P. L.; Thomson, W.; Willison, D. *J. Organomet. Chem.* **1988**, *354*, 233–242.
(11) Sugihara, T.; Yamaguchi, M. *Synlett* **1998**, 1384–1386.
(12) (a) Hanson, B. E. *Comments Inorg. Chem.* **2002**, *23*, 289–318. (b) Wang, H.; Sawyer, J. R.; Evans, P. A.; Baik, M-J. *Angew. Chem., Int. Ed. Engl.* **2008**, *47*, 342–345. (c) Pagenkopf, B. L.; Livinghouse, T. *J. Am. Chem. Soc.* **1996**, *118*, 2285–2286.
(13) Morimoto, T.; Chatani, N.; Fukumoto, Y.; Murai, S. *J. Org. Chem.* **1997**, *62*, 3762–3765.
(14) Kobayashi, T.; Koga, Y.; Narasaka, K. *J. Organomet. Chem.* **2001**, *624*, 73–87.
(15) Jeong, N.; Ki Sung, B.; Sung Kim, J.; Bong Park, S.; Deok Seo, S.; Young Shin, J.; Yeol In, K.; KyungChoi, Y. *Pure Appl. Chem.* **2002**, *74*, 85–91.
(16) Mukai, C.; Uchiyama, M.; Hanaoka, M. *J. Chem. Soc., Chem. Commun.* **1992**, 1014–1015.
(17) Hoye, T. R.; Suriano, J. A. *J. Am. Chem. Soc.* **1993**, *115* (3), 1154–1156.
(18) Negishi, E.; Holmes, S. J.; Tour, J. M.; Miller, J. A.; Cederbaum, F. E.; Swanson, D. R.; Takahashi, T. *J. Am. Chem. Soc.* **1989**, *111*, 3336–3346.
(19) Pearson, A. J.; Dubbert, R. A. *J. Chem. Soc., Chem. Commun.* **1991**, 202–203.
(20) Pearson, A. J.; Dubbert, R. A. *Organometallics* **1994**, *13*, 1656–1661.
(21) Mastrorilli, P.; Nobile, C. F.; Paolillo, R.; Suranna, G. P. *J. Mol. Catal. A: Chem.* **2004**, *214*, 103–106.
(22) Magnus, P.; Exon, C.; Albaugh-Robertson, P. *Tetrahedron* **1985**, *41* (24), 5861–5869.
(23) Rautenstrauch, V.; Megard, P.; Conesa, J.; Kuster, W. *Angew. Chem., Int. Ed. Engl.* **1990**, *29*, 1413–1416.
(24) Yamanaka, M.; Nakamura, E. *J. Am. Chem. Soc.* **2001**, *123*, 1703–1708.
(25) Gordon, C. M.; Kiszka, M.; Dunkin, I. R.; Kerr, W. J.; Scott, J. S.; Gebicki, J. *J. Organomet. Chem.* **1998**, *554*, 147–154.

(26) Banide, E. V.; Muller-Bunz, H.; Manning, A. R.; Evans, P.; McGlinchey, M. J. *Angew. Chem., Int. Ed.* **2007**, *46*, 2907–2910.
(27) Pallerla, M. K.; Yap, G. P. A.; Fox, J. M. *J. Org. Chem.* **2008**, *73*, 6137–6141.
(28) de Bruin, T. J. M.; Milet, A.; Greene, A. E.; Gimbert, Y. *J. Org. Chem.* **2004**, *69*, 1075–1080.
(29) Krafft, M. E.; Scott, I. L.; Romero, R. H.; Feibelmann, S.; Van Pelt, C. E. *J. Am. Chem. Soc.* **1993**, *115*, 7199–7207.
(30) Verdaguer, X.; Vazquez, J.; Fuster, G.; Bernardes-Genisson, V.; Greene, A. E.; Moyano, A.; Pericas, M. A.; Riera, A. *J. Org. Chem.* **1998**, *63*, 7037–7052.
(31) Cabot, R.; Lledo, A.; Reves, M.; Riera, A.; Verdaguer, X. *Organometallics* **2007**, *26*, 1134–1142.
(32) Blackmond, D. G. *Angew. Chem., Int. Ed.* **2005**, *44*, 4302–4320.
(33) (a) Jackson, S. M.; Chisholm, D. M.; McIndoe, J. S.; Rosenberg, L. *Eur. J. Inorg. Chem.* **2011**, 327–330. (b) Santos, L. S., Ed. *Reactive Intermediates: MS Investigations in Solution*; Wiley-VCH: Weinheim, Germany, 2010.
(34) (a) Rylander, P. N., *Organic Syntheses with Noble Metal Catalysts*; Academic Press: New York, 1973. (b) Brandsma, L.; Vasilevsky, S. F.; Verkruijsse, H. D., *Application of Transition Metal Catalysts in Organic Synthesis*; Springer: New York, 1999. (c) Jones, W. H., Ed. *Catalysis in Organic Synthesis*; Academic Press: Toronto, 1980. (d) Heaton, B., Ed. *Mechanisms in Homogeneous Catalysis*; Wiley-VCH: Weinheim, Germany, 2005.
(35) Henderson, W.; Evans, C. *Inorg. Chim. Acta* **1999**, *294*, 183–192.
(36) Santos, L. S.; Rosso, G. B.; Pilli, R. A.; Eberlin, M. N. *J. Org. Chem.* **2007**, *72*, 5809–5812.
(37) (a) Decker, C.; Henderson, W.; Nicholson, B. K. *J. Chem. Soc., Dalton Trans.* **1999**, 3507–3513. (b) Farrer, N. J.; McDonald, R.; McIndoe, J. S. *Dalton Trans.* **2006**, 4570–4579.
(38) Farrer, N. J.; McDonald, R.; Piga, T.; McIndoe, J. S. *Polyhedron* **2010**, *29*, 254–261.
(39) Henderson, W.; Nicholson, B. K. *J. Chem. Soc., Chem. Commun.* **1995**, 2531–2532.
(40) Henderson, W.; McIndoe, J. S.; Nicholson, B. K.; Dyson, P. J. *J. Chem. Soc., Dalton Trans.* **1998**, 519–525.
(41) (a) Hinderling, C.; Adlhart, C.; Chen, P. *Angew. Chem., Int. Ed.* **1998**, *37*, 2685–2689. (b) Chisholm, D. M.; Oliver, A. G.; McIndoe, J. S. *Dalton Trans.* **2010**, *39*, 364–373.
(42) (a) Adlhart, C.; Chen, P. *Helv. Chim. Acta* **2000**, *83*, 2192–2196. (b) Crawford, E.; Lohr, T.; Leitao, E. M.; Kwok, S.; McIndoe, J. S. *Dalton Trans.* **2009**, 9110–9112.
(43) Gimbert, Y.; Lesage, D.; Milet, A.; Fournier, F.; Greene, A. E.; Tabet, J. C. *Org. Lett.* **2003**, *5*, 4073–4075.
(44) Fei, Z.; Zhao, D.; Scopelliti, R.; Dyson, P. J. *Organometallics* **2004**, *23*, 1622–1628.
(45) (a) Butcher, C. P. G.; Dyson, P. J.; Johnson, B. F. G.; Khimyak, T.; McIndoe, J. S. *Chem. Eur. J.* **2003**, *9*, 944–950. (b) Crawford, E.; Dyson, P. J.; Forest, O.; Kwok, S.; McIndoe, J. S. *J. Cluster Sci.* **2006**, *17*, 47–63.
(46) Henderson, M. A.; Kwok, S.; McIndoe, J. S. *J. Am. Soc. Mass Spectrom.* **2009**, *20*, 658–666.
(47) Billington, D. C.; Helps, M. I.; Pauson, P. L.; Thomson, W.; Willison, D. *J. Organomet. Chem.* **1998**, *354*, 233–242.
(48) Vikse, K. L.; Woods, M. P.; McIndoe, J. S. *Organometallics* **2010**, *29*, 6615–6618.
(49) Vikse, K. L.; Ahmadi, Z.; Manning, C. C.; Harrington, D. A.; McIndoe, J. S. *Angew. Chem., Int. Ed.* **2011**, *50*, 8304–8306.
(50) Allian, A. D.; Tjahjono, M.; Garland, M. *Organometallics* **2006**, *25*, 2182–2188.
(51) Pearson, A. J.; Shively, R. J., Jr.; Dubbert, R. A. *Organometallics* **1992**, *11*, 4096–4104.
(52) Maryanoff, B. E.; Zhang, H. C. *Arkivoc* **2007**, *7*, 7–35.
(53) Rausch, B. J.; Gleiter, R.; Rominger, F. *Dalton Trans.* **2002**, 2219–2226.
(54) Roy, S. K.; Basak, A. *Chem. Commun.* **2006**, 1646–1648.
(55) Pearson, A. J.; Shively, R. J., Jr. *Organometallics* **1994**, *13*, 578–584.
(56) Battaglia, L .P.; Delledonne, D.; Nardelli, M.; Predieri, G.; Chiusoli, G. P.; Costa, M.; Pelizzi, C. *J. Organomet. Chem.* **1989**, *363*, 209–222.
(57) Krafft, M. E.; Boñaga, L. V. R.; Hirosawa, C. *J. Org. Chem.* **2001**, *66*, 3004–3020.
(58) *APEX-II v 2008-1*, Bruker AXS, Madison, WI.
(59) Sheldrick, G. M. *SADABS*; University of Göttingen, Göttingen, Germany, 2008. Sheldrick, G. M. *XPREP*; University of Göttingen, Göttingen, Germany, 2008.
(60) Sheldrick, G. M. *Acta Crystallogr.* **2008**, *A64*, 112.
(61) Farrugia, L. J. *J. Appl. Crystallogr.* **1997**, *30*, 565.
(62) http://www.povray.org/
(63) De Vynck, V.; Goethals, E. J. *Macromol. Rapid Commun.* **1997**, *18*, 149–156.